






## Variation in crystalline architectures through supramolecular interactions in copper(II) complexes with tridentate N<sub>2</sub>O donor Schiff bases

Subrata Jana, Partha Pratim Jana & Shouvik Chattopadhyay

To cite this article: Subrata Jana, Partha Pratim Jana & Shouvik Chattopadhyay (2015) Variation in crystalline architectures through supramolecular interactions in copper(II) complexes with tridentate N<sub>2</sub>O donor Schiff bases, *Journal of Coordination Chemistry*, 68:14, 2520-2538, DOI: [10.1080/00958972.2015.1043907](https://doi.org/10.1080/00958972.2015.1043907)


To link to this article: <http://dx.doi.org/10.1080/00958972.2015.1043907>

 View supplementary material 

 Accepted author version posted online: 23 Apr 2015.  
Published online: 14 Jun 2015.

 Submit your article to this journal 

 Article views: 99

 View related articles 

 View Crossmark data 

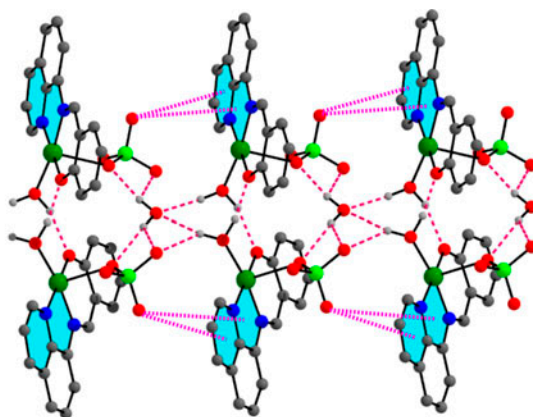
## Variation in crystalline architectures through supramolecular interactions in copper(II) complexes with tridentate N<sub>2</sub>O donor Schiff bases

SUBRATA JANA<sup>†</sup>, PARTHA PRATIM JANA<sup>‡,1</sup> and SHOUVIK CHATTOPADHYAY<sup>\*†</sup>

<sup>†</sup>Department of Chemistry, Inorganic Section, Jadavpur University, Kolkata, India

<sup>‡</sup>Centre for Analysis and Synthesis, Lund University, Lund, Sweden

(Received 25 August 2014; accepted 7 April 2015)



Three copper(II) complexes,  $[\text{Cu}(\text{L}^1)(\text{H}_2\text{O})(\text{ClO}_4)] \cdot 0.5\text{H}_2\text{O}$  (**1**),  $[\text{Cu}(\text{L}^2)(\text{H}_2\text{O})(\text{ClO}_4)] \cdot 0.5\text{H}_2\text{O}$  (**2**), and  $[\text{Cu}(\text{L}^3)(\text{NCNC}(\text{OCH}_3)\text{NH}_2)]\text{ClO}_4$  (**3**), where  $\text{HL}^1 = 4\text{-bromo-2-}(-(\text{quinolin-8-ylimino})\text{methyl})\text{phenol}$  and  $\text{HL}^2 = 1\text{-}(-(\text{quinolin-8-ylimino})\text{methyl})\text{naphthalen-2-ol}$ , have been prepared and characterized by elemental analysis, IR, UV–vis and fluorescence spectroscopy and single-crystal X-ray diffraction studies. The copper(II) centers assume five-coordinate square-pyramidal geometries in **1** and **2**, whereas square planar copper(II) is present in **3**. A methanol molecule has been inserted in the pendant end of the ligated dicyanamide in **3**. Various supramolecular architectures are formed by hydrogen bonding,  $\pi \cdots \pi$ ,  $\text{C-H} \cdots \pi$ , and  $\text{lp} \cdots \pi$  interactions.

**Keywords:** Copper(II); Schiff base; Crystal structure; Supramolecular interactions; Methanol insertion

### 1. Introduction

Transition metal complexes with Schiff bases play an important role in coordination chemistry related to catalysis and enzymatic reactions, magnetism, and molecular

\*Corresponding author. Email: [shouvik.chem@gmail.com](mailto:shouvik.chem@gmail.com)

<sup>1</sup>Present address: Department of Chemistry, Indian Institute of Technology, Kharagpur, India.

architectures [1, 2]. Focusing on supramolecular systems based on transition metal Schiff bases, one can find their potential uses as sensors, probes, photonic devices, catalysts, and in host–guest chemistry [3–9]. A significant number of supramolecular coordination complexes have been synthesized [10]. The most commonly used approach for engineering the crystal structure of such complexes employ non-covalent intermolecular forces (hydrogen bonding, aromatic ring stacking, etc.) [11, 12]. However, although there have been many reports on supramolecular systems, it still remains a difficult job to explore several complexes with different topological networks.

In this work, we have used two N<sub>2</sub>O donor Schiff bases, prepared by condensation of 5-bromosalicylaldehyde/2-hydroxynaphthaldehyde with 8-aminoquinoline, to prepare three new copper(II) complexes in the presence of different pseudohalides. Copper(II) assumes square planar/pyramidal geometry in the complexes. Herein, we report the syntheses, structural features, spectroscopic characterization, and X-ray crystal structures of three new complexes of copper(II). Different crystalline architectures are obtained via various supramolecular interactions, like H bonding,  $\pi\cdots\pi$ , C–H $\cdots\pi$ , and lp $\cdots\pi$  interactions. Another important observation is the insertion of methanol in the pendant end of ligated dicyanamide in one of the complexes.

## 2. Experimental

8-Aminoquinoline, 5-bromosalicylaldehyde, 2-hydroxy-1-naphthaldehyde, sodium dicyanamide, copper(II) perchlorate hexahydrate, and methanol were purchased from Sigma-Aldrich and were of reagent grade. They were used without purification.

*Caution!!!* Although no problems were encountered in this work, perchlorate salts containing organic ligands are potentially explosive. Only a small amount of the material should be prepared, and they should be handled with care.

### 2.1. Synthesis of HL<sup>1</sup>

The tridentate Schiff base HL<sup>1</sup> was synthesized by refluxing 8-aminoquinoline (1 mmol, 144 mg) with 5-bromosalicylaldehyde (1 mmol, 0.201 g) in methanol for ca. 1 h. The orange red solid was separated after one day by slow evaporation of the mother liquor. Red oil was collected from the reaction solution after drying on a vacuum pump. It was dissolved in diisopropyl ether, and red crystalline product was obtained after a few days.

Yield: 270 mg (82%). Anal. Calcd for C<sub>16</sub>H<sub>11</sub>BrN<sub>2</sub>O (FW 487.34): C, 58.74; H, 3.39; N, 8.56. Found: C, 58.65; H, 5.2; N, 9.0%. IR (KBr, cm<sup>-1</sup>): 1620 ( $\nu_{C=N}$ ), 3450 ( $\nu_{OH}$ ).

### 2.2. Synthesis of HL<sup>2</sup>

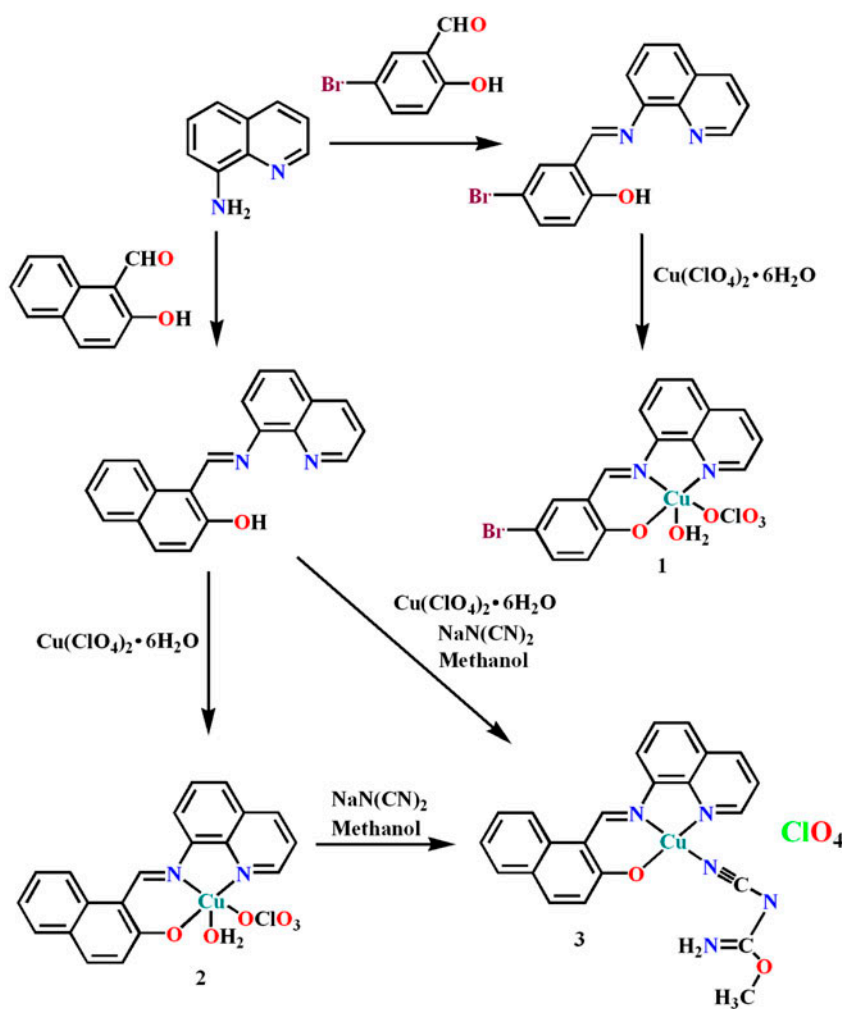
The tridentate Schiff base HL<sup>2</sup> was synthesized by refluxing 8-aminoquinoline (1 mmol, 144 mg) with 2-hydroxy-1-naphthaldehyde (1 mmol, 172 mg) in methanol for ca. 1 h. The orange red solid was separated after one day by slow evaporation of the mother liquor.

Yield: 300 mg (85%). Anal. Calcd for C<sub>20</sub>H<sub>14</sub>N<sub>2</sub>O (FW 298.34): C, 80.52; H, 4.73; N, 9.39. Found: C, 80.61; H, 4.68; N, 9.56%. IR (KBr, cm<sup>-1</sup>): 1628 ( $\nu_{C=N}$ ), 3440 ( $\nu_{OH}$ ).

### 2.3. Synthesis of $[Cu(L^1)(H_2O)(ClO_4)] \cdot 0.5H_2O$ (1)

A methanolic solution of copper(II) perchlorate hexahydrate (1 mmol, 370 mg) was added to methanolic solution of  $HL^1$  (1 mmol) and refluxed for ca. 1 h to get a green solution (scheme 1). Green single crystals, suitable for X-ray diffraction, were separated after a few days on slow evaporation of the reaction mixture in open atmosphere and collected by filtration.

Yield: 774 mg (75%). Anal. Calcd for  $C_{32}H_{26}Br_2Cl_2Cu_2N_4O_{13}$  (FW 1032.40): C, 37.23; H, 2.54; N, 5.43. Found: C, 37.21; H, 2.52; N, 5.49%. IR (KBr,  $cm^{-1}$ ): 1611 ( $\nu_{C=N}$ ), 1122 ( $\nu_{ClO_4}$ ), 3444 ( $\nu_{OH}$ ); UV-vis,  $\lambda_{max}$  (nm) [ $\epsilon_{max}$  ( $L mol^{-1} cm^{-1}$ )] (methanol) 333 (728), 456 (628). Magnetic moment: 1.71 BM.



Scheme 1. Synthesis of the complexes.

#### 2.4. Synthesis of $[Cu(L^2)(H_2O)(ClO_4)] \cdot 0.5H_2O$ (**2**)

Complex **2** was prepared in a similar method as for **1** except that  $HL^2$  (1 mmol) was used instead of  $HL^1$  (scheme 1). Black single crystals, suitable for X-ray diffraction, were obtained after a few days on slow evaporation of the methanol solution in open atmosphere.

Yield: 350 mg (71%). Anal. Calcd for  $C_{20}H_{16}ClCuN_2O_{6.5}$  (FW 487.34): C, 49.29; H, 3.31; N, 5.75. Found: C, 49.24; H, 3.33; N, 5.79%. IR (KBr,  $cm^{-1}$ ) 1615 ( $\nu_{C=N}$ ), 1121 ( $\nu_{ClO_4}$ ), 3435 ( $\nu_{OH}$ ); UV-vis,  $\lambda_{max}$  (nm) [ $\epsilon_{max}$  ( $L mol^{-1} cm^{-1}$ )] (methanol) 261 (1195), 348 (453), 478 (872). Magnetic moment: 1.73 BM.

#### 2.5. Synthesis of $[Cu(L^2)(NCNC(OCH_3)NH_2)]ClO_4$ (**3**)

A methanolic solution (10 mL) of copper(II) perchlorate hexahydrate (1 mmol, 370 mg) and sodium dicyanamide (1 mmol, 89 mg) was added to the methanolic solution of  $HL^2$  (1 mmol) and refluxed for 2 h (scheme 1). Black single crystals, suitable for X-ray diffraction, were obtained after a few days on slow evaporation of the reaction mixture in open atmosphere.

Alternatively, **3** was also prepared by the addition of a methanolic solution (5 mL) of sodium dicyanamide (1 mmol, 89 mg) to a methanolic solution (25 mL) of **2** (1 mmol, 487 mg) under reflux (scheme 1). Black single crystals, suitable for X-ray diffraction, were obtained after a few days on slow evaporation of the reaction mixture in open atmosphere.

Yield: 425 mg (76%). Anal. Calcd for  $C_{23}H_{18}ClCuN_5O_6$  (FW 559.42): C, 49.38; H, 3.24; N, 12.52. Found: C, 49.34; H, 3.21; N, 12.59%. IR (KBr,  $cm^{-1}$ ) 1600, 1614 ( $\nu_{C=N}$ ), 1121 ( $\nu_{ClO_4}$ ), 2194 ( $\nu_{C\equiv N}$ ); UV-vis,  $\lambda_{max}$  (nm) [ $\epsilon_{max}$  ( $L mol^{-1} cm^{-1}$ )] (methanol) 260 (1285), 348 (487), 478 (944). Magnetic moment: 1.70 BM.

#### 2.6. Physical measurements

Elemental analyses (carbon, hydrogen, and nitrogen) were performed using a PerkinElmer 240C elemental analyzer. IR spectra in KBr ( $4000\text{--}500 cm^{-1}$ ) were recorded using a PerkinElmer Spectrum Two FTIR spectrometer. Electronic spectra in methanol ( $800\text{--}200 nm$ ) were recorded in a PerkinElmer Lambda 35 UV-vis spectrophotometer. Fluorescence spectra were obtained on a Shimadzu RF-5301PC spectrofluorophotometer at room temperature. The magnetic susceptibility measurements were done with an EG and PAR vibrating sample magnetometer, model 155 at room temperature, and diamagnetic corrections were done using Pascal's constants.

#### 2.7. X-ray crystallography

Suitable crystals were picked, mounted on a glass fiber, and diffraction intensities were measured with an Oxford Diffraction XCalibur, Eos equipped with  $MoK\alpha$  radiation ( $\lambda = 0.71073 \text{ \AA}$ , 50 kV, 40 mA) at ambient temperature (293 K). Data collection and reduction were performed with the Oxford diffraction CrysAlis system. The structure solution and the refinement were carried out using the Jana 2006 program [13, 14]. Non-hydrogen atoms were refined anisotropically. Hydrogen atoms attached to oxygen and nitrogen atoms were located from difference Fourier maps and were kept fixed. Other hydrogens were placed in

their geometrically idealized positions and constrained to ride on their parent atoms. Significant crystallographic data are summarized in table 1.

## 2.8. Hirshfeld surface analysis

Hirshfeld surfaces [15–17] and the associated 2-D fingerprint [18–20] plots were calculated using Crystal Explorer [21] with bond lengths to hydrogens set to standard values [22]. For each point on the Hirshfeld isosurface, two distances  $d_e$ , the distance from the point to the nearest nucleus external to the surface and  $d_i$ , the distance to the nearest nucleus internal to the surface, are defined. The normalized contact distance ( $d_{\text{norm}}$ ) based on  $d_e$  and  $d_i$  is given by

$$d_{\text{norm}} = \frac{(d_i - r_i^{\text{vdw}})}{r_i^{\text{vdw}}} + \frac{(d_e - r_e^{\text{vdw}})}{r_e^{\text{vdw}}}$$

where  $r_i^{\text{vdw}}$  and  $r_e^{\text{vdw}}$  are the van der Waals radii of the atoms. The value of  $d_{\text{norm}}$  is negative or positive depending on intermolecular contacts being shorter or longer than the van der Waals separations. The parameter  $d_{\text{norm}}$  displays a surface with a red–white–blue color scheme, where bright red spots highlight shorter contacts, white areas represent contacts around the van der Waals separation, and blue regions are devoid of close contacts. For a given crystal structure and set of spherical atomic electron densities, the Hirshfeld surface is unique [23], and thus, it suggests the possibility of gaining additional insight into the intermolecular interaction of molecular crystals.

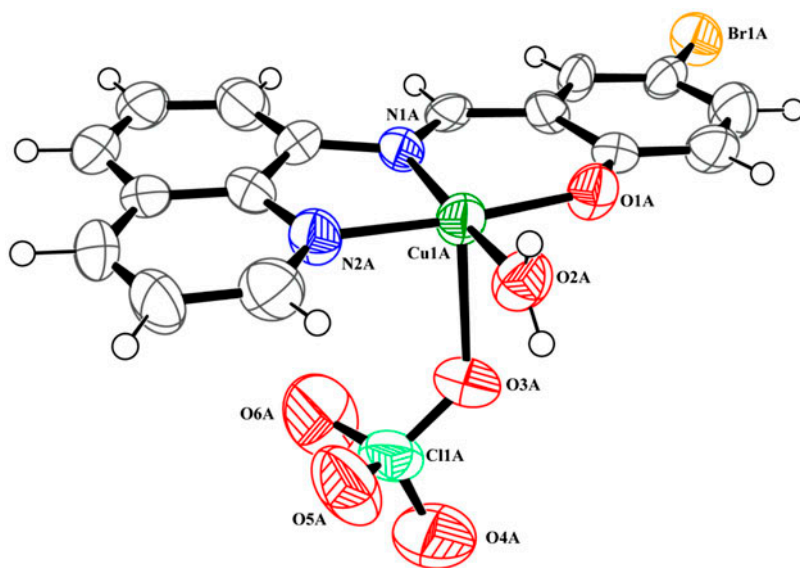


Figure 1. ORTEP view of **1A** with 50% ellipsoid probability. All non-C, H atoms are labeled. Water is not shown for clarity.

Table 1. Crystal data and refinement details of 1–3.

Complex	1	2	3
Formula	C <sub>32</sub> H <sub>24</sub> Br <sub>2</sub> Cl <sub>2</sub> Cu <sub>2</sub> N <sub>4</sub> O <sub>13</sub>	C <sub>20</sub> H <sub>16</sub> ClCuN <sub>2</sub> O <sub>6.5</sub>	C <sub>33</sub> H <sub>18</sub> ClCuN <sub>5</sub> O <sub>6</sub>
Formula weight	1032.40	487.34	559.42
Temperature (K)	293	293	293
Crystal system	Triclinic	Triclinic	Monoclinic
Space group	<i>P</i> - <i>1</i>	<i>P</i> - <i>1</i>	<i>P</i> 2 <sub>1</sub> / <i>n</i>
<i>a</i> (Å)	7.4619(6)	8.0770(4)	7.0444(3)
<i>b</i> (Å)	13.8993(11)	10.0784(5)	17.7753(8)
<i>c</i> (Å)	18.7383(17)	12.5840(6)	18.2335(8)
$\alpha$ (°)	92.654(7)	70.468(4)	(90)
$\beta$ (°)	100.938(7)	87.197(4)	98.438(4)
$\gamma$ (°)	104.590(7)	87.711(4)	(90)
<i>Z</i>	2	2	4
$d_{\text{calc}}$ (g cm <sup>-3</sup> )	1.862	1.676	1.645
$\mu$ (mm <sup>-1</sup> )	3.548	1.318	1.138
<i>F</i> (000)	1020	494	1140
Total reflections	26,293	7672	25,551
Unique reflections	8779	4324	5597
Observed data [ <i>I</i> > 2 $\sigma$ ( <i>I</i> )]	3060	3156	2990
No. of parameters	496	272	334
<i>R</i> (int)	0.117	0.027	0.076
<i>R</i> <sub>1</sub> , <i>wR</i> <sub>2</sub> (all data)	0.2265, 0.2561	0.0771, 0.1610	0.1598, 0.1736
<i>R</i> <sub>1</sub> , <i>wR</i> <sub>2</sub> [ <i>I</i> > 2 $\sigma$ ( <i>I</i> )]	0.0852, 0.1839	0.0523, 0.1411	0.0763, 0.1436
Min. and max. resd. dens.	1.39, -1.24	1.09, -0.47	0.58, -0.34

## 2.9. Theoretical calculations

All theoretical calculations of molecule geometry were created using the atomic coordinates obtained from X-ray geometry. Geometry optimizations of all the complexes were performed using density functional theory at the B3LYP level using the GAUSSIAN 03 W suite of programs [24–27]. The geometries of the complexes were fully optimized in gas phase without any symmetry constraints. All subsequent calculations were carried out based on the optimized structure. For C, H, N, O, and Cl, the 6-31G (d, p) basis sets were used, while for copper(II), the LANL2DZ basis set was employed [28–30].

## 3. Results and discussion

### 3.1. Synthesis

The tridentate Schiff bases, HL<sup>1</sup> and HL<sup>2</sup>, were prepared by 1 : 1 condensation of 8-aminoquinoline with 5-bromosalicylaldehyde and 2-hydroxy-1-naphthaldehyde, respectively, following the literature method [31]. HL<sup>1</sup> and HL<sup>2</sup> on reaction with copper(II) perchlorate hexahydrate produce **1** and **2**, respectively. Complex **3** was prepared by reaction with the Schiff base ligand, HL<sup>2</sup>, copper(II) perchlorate, and sodium dicyanamide in methanol. It is interesting that a methanol molecule was inserted to the terminal C≡N of dicyanamide in **3**. Insertion of methanol into the C≡N bond of dicyanamide was also observed in other complexes [32–36]. Two methanol molecules have been inserted into two C≡N bonds of a dicyanamide in all such complexes, which are shown in table 2. There is not a single example where one methanol is inserted into one C≡N bond of a dicyanamide. Complex **3** is therefore the first example of a transition metal complex, where only one methanol has been inserted into one C≡N bond of a coordinated dicyanamide. It is to be noted here that **3** could also be produced by addition of a methanolic solution of sodium dicyanamide into the methanolic solution of **2**. The formation of the complexes is shown in scheme 1.

### 3.2. Description of the structures

**3.2.1. [Cu(L<sup>1</sup>)(H<sub>2</sub>O)(ClO<sub>4</sub>)]·0.5H<sub>2</sub>O (**1**).** The structure of **1** contains two independent units (**A** and **B**) and one lattice water. A perspective view of molecules **A** and **B** are shown together with the atom numbering scheme in figures 1 and S1 (see online supplemental material at <http://dx.doi.org/10.1080/00958972.2015.1043907>), respectively. Complex **1** crystallizes in triclinic space group *P*-1. The Addison parameter (trigonality index,  $\tau = (\alpha - \beta)/60$ , where  $\alpha$  and  $\beta$  are the two largest L–M–L angles of the coordination sphere) is 0.055 and 0.083 in **A** and **B**, respectively, and this confirms the square-pyramidal character ( $\tau = 0$  for a perfect square pyramid and a  $\tau = 1$  for a perfect trigonal bipyramid) [37]. The copper(II) center is coordinated equatorially by a phenoxo oxygen, O(1), a pyridine nitrogen, N(1), and one imine nitrogen, N(2), of the tridentate deprotonated Schiff base and one water oxygen, O(2). The apical position is occupied by one perchlorate oxygen, O(3), to complete the square-pyramidal geometry of copper(II) [some related coordinating perchlorate oxygen distances from CSD are given in table S1 (Electronic Supplementary Information)]. As usual for a square pyramid structure, the copper(II) center is slightly pulled out of the least-squares plane toward the apical donor at a distance 0.091(1) Å in **A** and 0.10(1) Å in **B**. Deviations of the coordinating atoms, N(1), N(2), O(1), and O(2) from the



Table 2. Selected complexes containing methanol-inserted dicyanamide.

Complexes	Ref.
Cu(NHC(OCH <sub>3</sub> )NHNHC(OCH <sub>3</sub> ) <sub>2</sub> )	[32]
[Cu(HdcaMeOH) <sub>2</sub> ](ClO <sub>4</sub> ) <sub>2</sub> ·2H <sub>2</sub> O	[34]
HdcaMeOH = (methoxycarbimido)cyanamide	
[Cu <sub>2</sub> (CH <sub>3</sub> O) <sub>2</sub> (C <sub>4</sub> H <sub>8</sub> N <sub>3</sub> O <sub>2</sub> ) <sub>2</sub> ]	[35]
[Cu(ClO <sub>4</sub> ) <sub>2</sub> (C <sub>4</sub> H <sub>9</sub> N <sub>3</sub> O <sub>2</sub> ) <sub>2</sub> ][Cu(C <sub>4</sub> H <sub>9</sub> N <sub>3</sub> O <sub>2</sub> ) <sub>2</sub> (CH <sub>3</sub> O) <sub>2</sub> ](ClO <sub>4</sub> ) <sub>2</sub> ·2CH <sub>3</sub> O	[36]

least-squares basal plane passing through them are  $-0.040(9)$ ,  $0.041(8)$ ,  $-0.039(7)$ , and  $0.038(7)$  Å, respectively, in **A** and  $-0.044(9)$ ,  $0.045(8)$ ,  $-0.043(7)$ , and  $0.042(7)$  Å, respectively, in **B**. The bond lengths in the equatorial plane are very similar in the two independent units. Selected bond lengths and angles are given in table 3. Cu–O distances range from 1.914(7) to 2.015(4) Å, while the Cu–N distances are 1.980(8)–1.995(8) Å. The Cu–O and Cu–N distances are comparable with previously reported complexes [38–41]. Tables 4 and 5 contain Cu–O and Cu–N distances in selected complexes, respectively.

The hydrogens, H(2C) and H(2D), attached to O(2B) are involved in hydrogen bonding interactions with the symmetry-related phenoxo oxygen, O(1A)<sup>b</sup> (<sup>b</sup> =  $x, y, 1 + z$ ) and symmetry-related perchlorate oxygen, O(6B)<sup>a</sup> (<sup>a</sup> =  $2 - x, 1 - y, -z$ ), respectively. Similarly, H(2F) attached to O(2A) is involved in hydrogen bonding interaction with the symmetry-related phenoxo oxygen, O(1B)<sup>c</sup> (<sup>c</sup> =  $x, y, -1 + z$ ). The combination of all the above hydrogen bonding interactions forms a supramolecular chain along the crystallographic *a* axis (figure 2). Details of the hydrogen bonding interactions are given in table 6.

The perchlorate oxygen, O(5A), attached to Cl(1A) is involved in intermolecular  $lp \cdots \pi$  interaction with symmetry-related six-membered ( $2 - x, 1 - y, -z$ ) pyridine ring, N(2A)–C(15A)–C(14A)–C(13A)–C(12A)–C(16A), to form a supramolecular chain along the crystallographic *a* axis, as shown in figure 2. Similarly, the perchlorate, O(5B), attached to Cl(1B) is involved in intermolecular  $lp \cdots \pi$  interaction with six-membered ( $2 - x, -y, -z$ )

Table 3. Selected bond lengths (Å) and angles (°) for **1–3**.

	1			2		3	
	Exp.(A)	Exp.(B)	Cal.	Exp.	Cal.	Exp.	Cal.
Cu(1)–O(1)	1.901(7)	1.916(7)	1.895	1.885(2)	1.888	1.898(3)	1.857
Cu(1)–O(2)	1.986(7)	2.003(8)	2.016	1.976(3)	2.081	–	–
Cu(1)–O(3)	2.442(8)	2.483(9)	2.248	2.655(4)	2.207	–	–
Cu(1)–N(1)	1.981(8)	1.960(8)	1.999	1.938(3)	1.953	1.934(4)	1.910
Cu(1)–N(2)	1.985(8)	1.990(9)	1.954	1.981(4)	1.990	1.972(4)	1.965
Cu(1)–N(3)	–	–	–	–	–	1.985(5)	2.008
O(1)–Cu(1)–O(2)	88.5(3)	89.0(3)	84.52	89.29(11)	84.03	–	–
O(1)–Cu(1)–N(1)	93.7(3)	93.9(3)	93.82	92.72(14)	91.04	92.44(15)	95.14
O(1)–Cu(1)–N(2)	175.2(3)	175.8(3)	159.75	176.52(14)	169.94	175.64(15)	161.79
O(1)–Cu(1)–N(3)	–	–	–	–	–	88.79(19)	89.07
O(1)–Cu(1)–O(3)	91.2(3)	90.7(3)	84.52	96.14(12)	101.33	–	–
O(2)–Cu(1)–N(1)	171.9(3)	170.8(3)	167.17	174.41(13)	95.49	–	–
O(2)–Cu(1)–N(2)	94.5(3)	93.2(3)	93.82	94.07(12)	144.04	–	–
O(2)–Cu(1)–O(3)	89.0(3)	90.2(3)	88.92	81.01(12)	84.03	–	–
N(1)–Cu(1)–N(2)	82.8(4)	83.5(4)	83.32	83.86(14)	83.43	83.89(15)	85.61
N(1)–Cu(1)–N(3)	–	–	–	–	–	177.4(2)	156.22
N(2)–Cu(1)–N(3)	–	–	–	–	–	94.98(19)	97.56
O(3)–Cu(1)–N(1)	98.8(3)	98.5(3)	103.85	103.94(13)	123.16	–	–
O(3)–Cu(1)–N(2)	92.6(3)	92.9(3)	98.54	85.28(12)	88.71	–	–

Table 4. Selected copper(II)–nitrogen distances (Å) in some reported complexes.

Complexes	Bond distance (Å)		Ref.
<b>1A</b>	1.981(8)	1.985(8)	This work
<b>1B</b>	1.960(8)	1.990(9)	This work
<b>2</b>	1.938(3)	1.981(4)	This work
<b>3</b>	1.934(4)	1.972(4)	This work
[Cu(L <sup>1</sup> )(bpy)], H <sub>2</sub> L <sup>1</sup> = 2-({2-[(2-carboxybenzoyl)-xy]ethoxy}carbonyl)benzoic acid	1.977(2)	2.000(2)	[38]
[Cu(L <sup>1</sup> )(phen)]·DMF	1.987(5)	2.016(5)	[38]
[Cu(mqmp)(H <sub>2</sub> O) <sub>2</sub> ](ClO <sub>4</sub> ), mqmp = 2-methoxy-6-((quinolin-8-ylimino)methyl)phenol	1.954(2)	1.987(2)	[39]
[Cu <sub>2</sub> (mqmp) <sub>2</sub> Cl <sub>2</sub> ]	1.968(2)	1.999(2)	[39]
[Cu <sub>2</sub> (L <sup>1</sup> ) <sub>2</sub> (N <sub>3</sub> ) <sub>2</sub> (ClO <sub>4</sub> ) <sub>2</sub> ], L <sup>1</sup> = N,N-dimethyl-N'-(1-pyridin-2-yl-ethylidene)-ethane-1,2-diamine	1.944(3)	2.021(2)	[40]
[Cu <sub>2</sub> (L <sup>2</sup> ) <sub>2</sub> (NCS) <sub>2</sub> ](ClO <sub>4</sub> ) <sub>2</sub> , L <sup>2</sup> = N,N-diethyl-N'-(1-pyridin-2-yl-ethylidene)-ethane-1,2-diamine	1.943(2)	2.017(2)	[40]

pyridine ring, N(2B)–C(15B)–C(14B)–C(13B)–C(12B)–C(16B), to form a supramolecular chain along the crystallographic *a* axis, as shown in figure 2. Geometric features of the lp⋯π interactions are given in table 7.

**3.2.2. [Cu(L<sup>2</sup>)(H<sub>2</sub>O)(ClO<sub>4</sub>)]·0.5H<sub>2</sub>O (2).** Complex **2** crystallizes in triclinic space group *P*-1. The asymmetric unit consists of discrete mononuclear copper(II) complex and solvent water. A perspective view of **2** with atom numbering scheme is shown in figure 3. Selected bond lengths and angles are shown in table 3. The copper(II) center has a five-coordinate square-pyramidal geometry, as confirmed by the value of the Addison parameter (0.041). Cu(1) is coordinated equatorially by one phenoxo oxygen, O(1), one imine nitrogen, N(1), and one pyridine nitrogen, N(2), of the tridentate deprotonated Schiff base ligand and one

Table 5. Selected copper(II)–oxygen distances (Å) in some reported complexes.

Complexes	Bond distance (Å)		Ref.
<b>1A</b>	1.901(7)	1.986(7)	This work
<b>1B</b>	1.916(7)	2.003(8)	This work
<b>2</b>	1.885(2)	1.976(3)	This work
<b>3</b>	1.898(3)		This work
[Cu(L <sup>1</sup> )(bpy)], H <sub>2</sub> L <sup>1</sup> = 2-({2-[(2-carboxybenzoyl)-xy]ethoxy}carbonyl)benzoic acid	1.9532(18)	1.9623(19)	[38]
[Cu(L <sup>1</sup> )(phen)]·DMF	1.9084(19)	1.9938(19)	[38]
[Cu(mqmp)(H <sub>2</sub> O) <sub>2</sub> ](ClO <sub>4</sub> ), mqmp = 2-methoxy-6-((quinolin-8-ylimino)methyl)phenol	1.898(1)	1.978(2)	[39]
[Cu <sub>2</sub> (mqmp) <sub>2</sub> Cl <sub>2</sub> ]	1.900(1)		[39]
pyCu(phenylacetate) <sub>4</sub> Cupy	1.971(2)	1.981(2)	[41]
[Cu <sub>2</sub> (3-MePhCOO) <sub>4</sub> (NITmPy) <sub>2</sub> ], NITmPy = 2-(3-pyridyl)-4,4,5,5-tetramethyl-4,5-dihydro 1H-imidazolyl-1-oxyl-3-oxide	1.967(3)	1.953(3)	[41]

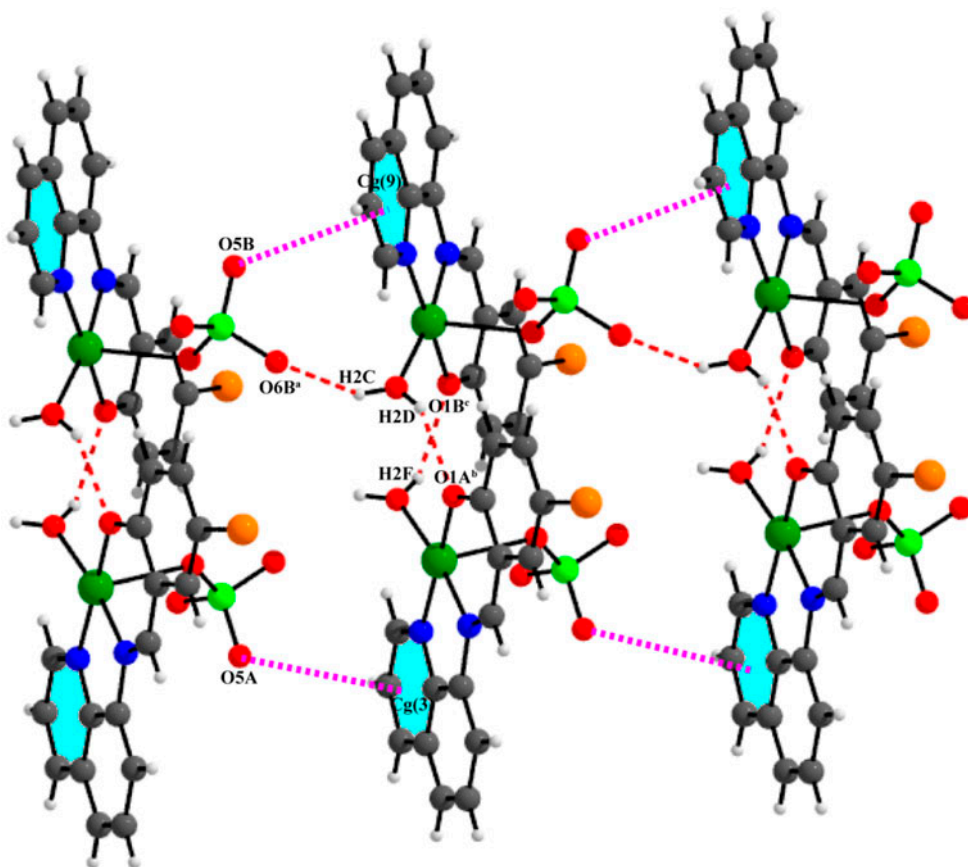


Figure 2. 1-D supramolecular chain of **1** via hydrogen bonding and  $lp \cdots \pi$  interactions. Hydrogen bonds are shown as red dotted lines and  $lp \cdots \pi$  interactions are shown by magenta dotted lines (see <http://dx.doi.org/10.1080/00958972.2015.1043907> for color version).

water oxygen, O(2). The apical position is occupied by one perchlorate oxygen, O(3), to complete the square-pyramidal geometry of Cu(1). Deviations of the coordinating atoms, N(1), N(2), O(1), and O(2), from the least-squares basal plane are  $-0.040(2)$ ,  $0.042(2)$ ,  $-0.040(2)$ , and  $0.039(2)$  Å, respectively, and that of the copper(II) from the same plane toward the apical donor oxygen is  $0.0519(4)$  Å. Cu–O distances are  $1.885(2)$ – $2.655(4)$  Å, while the Cu–N distances are  $1.938(3)$ – $1.981(4)$  Å. The Cu–O and Cu–N distances are comparable with previously reported complexes [38–41]. Tables 4 and 5 contain Cu–O and Cu–N distances in selected complexes, respectively. H(1) and H(2), attached to O(2), are involved in hydrogen bonding interactions with the symmetry-related perchlorate oxygen, O(6)<sup>g</sup> ( $^g = 1 - x, 1 - y, -z$ ) and phenoxo oxygen, O(1)<sup>h</sup> ( $^h = -x, -y, -z$ ), respectively, to form a supramolecular dimer, as shown in figure 4. Details about the hydrogen bonds are given in table 6. The unsaturated pyridine ring N(2)–C(19)–C(18)–C(17)–C(16)–C(20) is involved in intermolecular  $\pi \cdots \pi$  interactions with symmetry-related  $(-x, -y, 1 - z)$  pyridine ring N(2)–C(19)–C(18)–C(17)–C(16)–C(20), and phenyl rings C(4)–C(5)–C(6)–C(7)–C(8)–C(9) and C(12)–C(13)–C(14)–C(15)–C(16)–C(20), forming a 1-D chain, as shown in figure 5. Geometric features of the  $\pi \cdots \pi$  interactions are given in table 8.

Table 6. Hydrogen bond distances (Å) and angles (°) of 1–3.

Complexes	D–H···A	D–H	D···A	H···A	∠D–H···A
1	O(2B)–H(2C)···O(6B) <sup>a</sup>	0.82	2.943(13)	2.29	137
	O(2B)–H(2D)···O(1A) <sup>b</sup>	0.82	2.702(10)	2.05	136
	O(2A)–H(2F)···O(1B) <sup>c</sup>	0.82	2.791(10)	2.15	134
2	O(2)–H(1)···O(6) <sup>d</sup>	0.82	2.815(4)	2.00	173
	O(2)–H(2)···O(1) <sup>e</sup>	0.82	2.701(4)	2.25	115
3	N(5)–H(5A)···O(1)	0.87	3.00(6)	2.15(7)	165(6)
	N(5)–H(5B)···O(6) <sup>f</sup>	0.86	3.087(9)	2.23(6)	175(4)

Note: Symmetry transformations: <sup>a</sup> = 2 – x, 1 – y, –z; <sup>b</sup> = x, y, 1 + z; <sup>c</sup> = x, y, –1 + z; <sup>d</sup> = 1 – x, 1 – y, –z; <sup>e</sup> = –x, –y, –z; <sup>f</sup> = –x, 1 – y, –z.

**3.2.3. [Cu(L<sup>2</sup>)(NCNC(OCH<sub>3</sub>)NH<sub>2</sub>)]ClO<sub>4</sub> (3).** A perspective view of **3** with atom numbering is shown in figure 6. **3** crystallizes in monoclinic space group *P2<sub>1</sub>/n*. The copper(II) center has four-coordinate square planar geometry. Cu(1) is coordinated by one phenoxo oxygen, O(1), one pyridine nitrogen, N(2), and one imine nitrogen, N(1), of the tridentate deprotonated Schiff base ligand and one nitrogen, N(3), from a dicyanamide. A methanol is inserted into the terminal unsaturated C≡N bond of dicyanamide. Selected bond lengths and angles are shown in table 3. Deviations of the coordinating atoms, O(1), N(1), N(2), and N(3), from the least-squares mean plane through them are –0.038(3), –0.038(4), 0.040(4), and 0.036(4) Å, respectively, and that of Cu(1) from the same plane is 0.0002(6) Å. Cu–O distances are 1.898(3) Å, while the Cu–N distances are 1.934(4)–1.985(5) Å. The Cu–O and Cu–N distances are comparable with previously reported complexes [38–41]. Tables 4 and 5 contain Cu–O and Cu–N distances in selected complexes, respectively.

H(5A), attached to N(5), is involved in intramolecular hydrogen bonding interaction with the phenoxo oxygen, O(1), to form an eight-membered supramolecular ring, as shown in figure 7. Similarly, H(5B), attached to N(5), is involved in intermolecular hydrogen bonding interaction with the symmetry-related (*x*, 1 – *y*, –*z*) perchlorate oxygen, O(6). Details of the hydrogen bonding interaction are given in table 6. One methyl hydrogen, H(23 C), attached to C(23) is involved in an intermolecular C–H···π interaction with the symmetry-related (1/2 – *x*, –1/2 + *y*, 1/2 – *z*) pyridine ring N(2)–C(20)–C(16)–C(17)–C(18)–C(19), forming a chain along the crystallographic *b* axis (figure 8). The six-membered pyridine ring N(2)–C(20)–C(16)–C(17)–C(18)–C(19) is involved in intermolecular π···π interaction with symmetry-related (1 – *x*, 1 – *y*, –*z*) phenyl ring C(4)–C(5)–C(6)–C(7)–C(8)–C(9), forming a supramolecular dimer (figure 9). Geometric features of π···π and C–H···π interactions are given in tables 8 and 9, respectively.

**3.2.4. Intermolecular interactions of the three molecular crystal lattices.** All three complexes show hydrogen bonding interactions. Complex **1** forms a 1-D supramolecular chain along the crystallographic *a* axis via intermolecular hydrogen bonding interactions, whereas

Table 7. Geometric features of the lp···π interactions obtained for 1.

Y–X···Cg(Ring)	X···Cg (Å)	Y–X···Cg (°)	Y···Cg (Å)	Symmetry transformation
Cl(1A)–O(5A)···Cg(3)	3.779(16)	115.6(7)	4.573(6)	2 – x, 1 – y, –z
Cl(1B)–O(5B)···Cg(9)	3.661(14)	122.7(7)	4.572(6)	2 – x, 1 – y, –z

Note: Cg(3) = center of gravity of ring [N(2A)–C(15A)–C(14A)–C(13A)–C(12A)–C(16A)]; Cg(9) = center of gravity of ring [N(2B)–C(15B)–C(14B)–C(13B)–C(12B)–C(16B)].

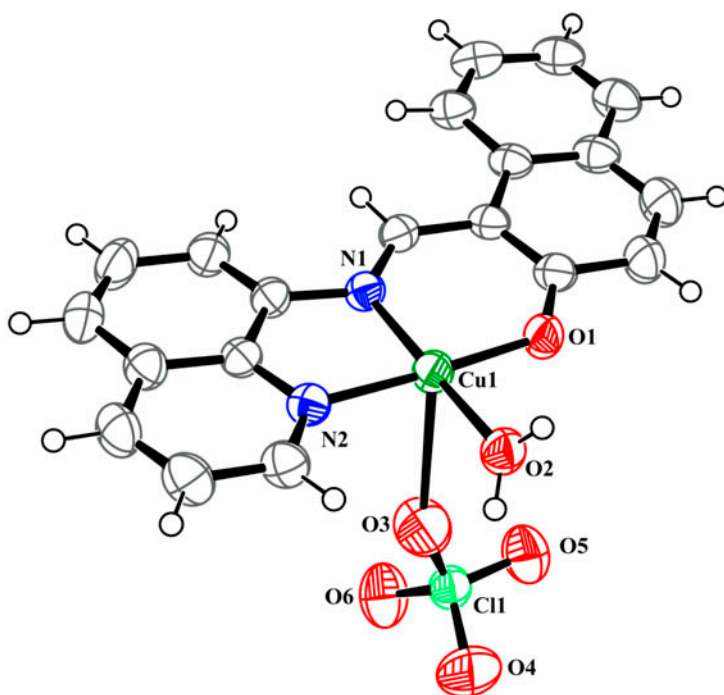


Figure 3. ORTEP view of **2** with 50% ellipsoid probability. All non-C, H atoms are labeled. Water is not shown for clarity.

**2** forms a supramolecular dimer via hydrogen bonding. Complex **3** forms intramolecular hydrogen bonds. Complex **1** shows  $lp \cdots \pi$  interaction to form a supramolecular chain along the crystallographic  $a$  axis. Complexes **2** and **3** show  $\pi \cdots \pi$  interactions. Complex **2** forms a supramolecular 1-D chain via  $\pi \cdots \pi$  interactions, whereas **3** forms a supramolecular dimer via  $\pi \cdots \pi$  interactions. Complex **1** forms a supramolecular 1-D chain via  $C-H \cdots \pi$  interactions. Complexes **2** and **3** do not have any  $C-H \cdots \pi$  interactions.

### 3.3. Hirshfeld surface analysis

The Hirshfeld surfaces mapped with  $d_{\text{norm}}$  for **1**, **2**, and **3** are illustrated in figures S2–S4 (Supplementary Information), respectively. The dominant interactions between  $O \cdots H$ ,  $Br \cdots H$ , and  $Cl \cdots H$  in all the complexes can be seen in the Hirshfeld surface as the bright red areas. Other visible spots in the Hirshfeld surfaces correspond to  $H \cdots H$  contacts. The small extent of area and light color on the surface indicates weaker and longer contacts other than hydrogen bonds. 2-D fingerprint plots complement these surfaces, quantitatively summarizing the nature and type of intermolecular contacts experienced by the molecules in the crystal. The  $O \cdots H/H \cdots O$  intermolecular interactions appear as distinct spikes in the 2-D fingerprint plots of all three complexes. The fingerprint plots can be decomposed to highlight particular close contacts [42]. This decomposition enables the separation of contributions from different interaction types, which overlap in the full fingerprint. The amount of  $O \cdots H/H \cdots O$  interactions comprises 29.5, 36.8 and 26.4% of the Hirshfeld surfaces for each molecule of **1**, **2**, and **3**, respectively. The  $O \cdots H$  interaction is represented by a spike

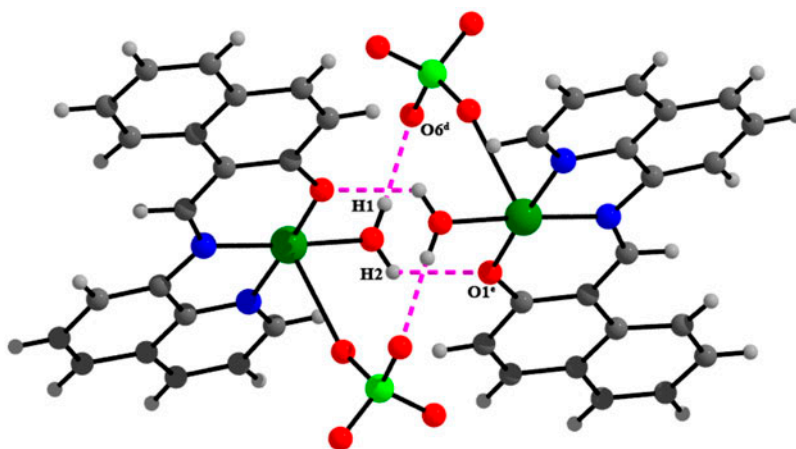


Figure 4. Hydrogen-bonded dimer of **2**. Hydrogen bonds are shown as dotted lines.

( $d_i = 1.06$ ,  $d_e = 0.66$  Å in **1**,  $d_i = 1.06$ ,  $d_e = 0.73$  Å in **2** and  $d_i = 1.34$ ,  $d_e = 1.06$  Å in **3**) in the bottom left (donor) area of the fingerprint plot (figures S2c, S3c and S4c, Supplementary Information). The  $H \cdots O$  interaction is also represented by another spike ( $d_i = 0.72$ ,  $d_e = 1.12$  Å in **1**,  $d_i = 0.73$ ,  $d_e = 1.06$  Å in **2** and  $d_i = 1.06$ ,  $d_e = 1.34$  Å in **3**) in the bottom right (acceptor) region of the fingerprint plot and can be viewed as bright red spots on the  $d_{\text{norm}}$  surface.

### 3.4. Geometry optimization

The calculated geometrical parameters (bond lengths and bond angles) of the complexes were given with the experimental ones in table 3 and are in agreement with the

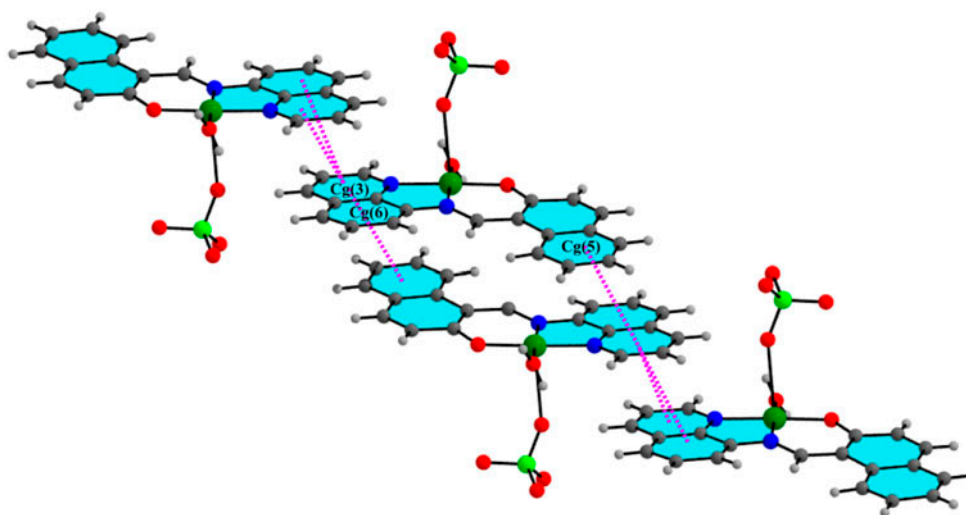


Figure 5. 1-D chain of **2** via  $\pi \cdots \pi$  interactions.

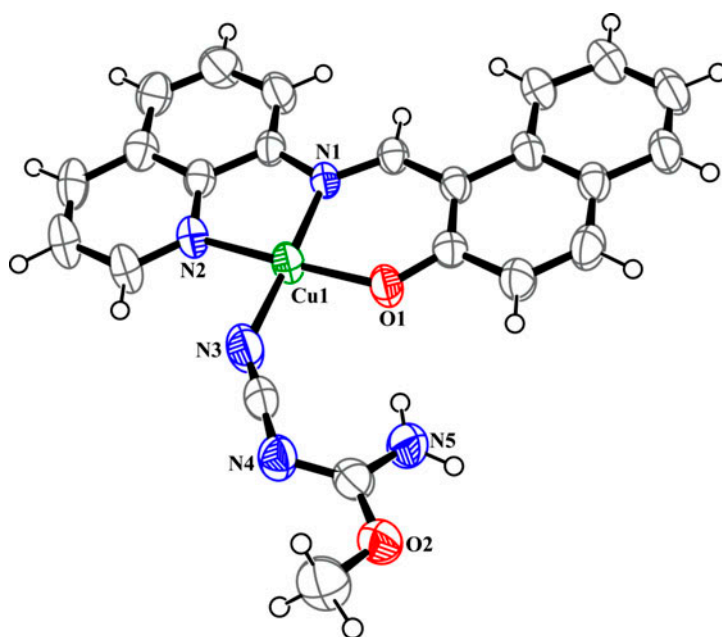


Figure 6. ORTEP view of **3** with 50% ellipsoid probability. All non-C, H atoms are labeled. Perchlorate is not shown for clarity.

experimental values. The HOMO energy levels vary from  $-2.04$  to  $-2.17$  eV, while the LUMO energy levels are very close, with energies ranging from  $-0.097$  to  $-1.06$  eV. The HOMO-LUMO energy gaps are 0.111, 0.112, and 0.107 eV in **1**, **2**, and **3**, respectively. The frontier molecular orbitals and their respective positive and negative regions of all the complexes are shown in figure S5 (Supplementary Information). The positive and negative phases are represented in red and blue, respectively.

### 3.5. IR and UV-vis spectra, fluorescence, and magnetic moment

In the IR spectra of all three complexes, distinct bands due to azomethine (C=N) groups at  $1600$ – $1615$   $\text{cm}^{-1}$  were present [40]. The C=N stretches of ligands were observed at  $1620$ – $1630$   $\text{cm}^{-1}$ . The lowering of C=N stretches in complexes is due to coordination to copper (II) [43]. IR spectra of **1** and **2** displayed broad bands from  $1070$  to  $1144$   $\text{cm}^{-1}$ , splitting into three peaks assigned to the presence of coordinated perchlorate, as also supported by the crystal structure [40]. The band at  $1122$   $\text{cm}^{-1}$  in **3** is devoid of splitting and is consistent with the IR active normal mode for  $T_d$  symmetry, suggesting that the anion is not coordinated to copper(II) as substantiated by the crystal structure. In IR spectra of **3**, the appearance of a strong band at  $2194$   $\text{cm}^{-1}$  indicated the presence of C≡N in the methanol-inserted dicyanamide [44]. Broad bands at  $3365$ – $3444$   $\text{cm}^{-1}$  were observed due to OH stretch for **1** and **2** [44].

The electronic spectra in methanol are recorded in the range  $200$ – $800$  nm (figure 10). The intense absorption bands at short wavelengths,  $300$ – $500$  nm, may be assigned to ( $n$ - $\pi^*$ ) and ( $\pi$ - $\pi^*$ ) transitions [45]. The absorptions at  $750$  nm may be assigned to d-d transitions [41].

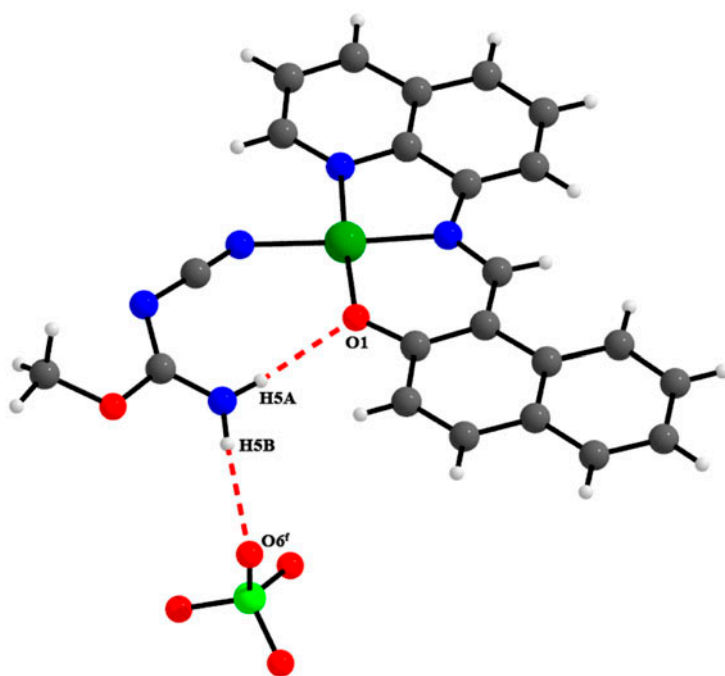


Figure 7. Hydrogen-bonded structure of **3**.

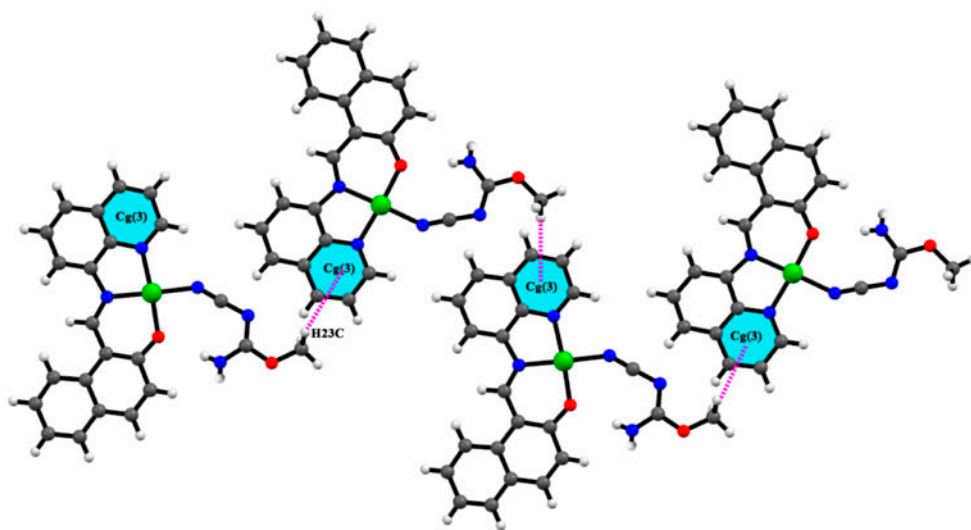


Figure 8. 1-D chain of **3** via C-H... $\pi$  interactions.



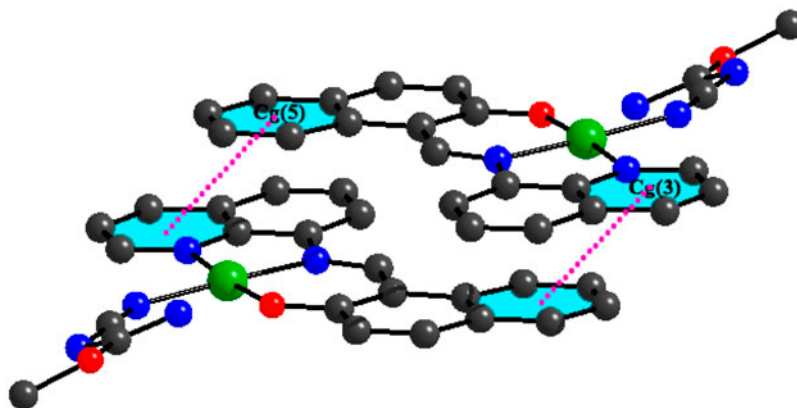


Figure 9. Supramolecular dimer of **3** via  $\pi \cdots \pi$  interactions. Hydrogens are not shown for clarity.

Table 8. Geometric features of the  $\pi \cdots \pi$  interactions obtained for **2** and **3**.

Complex	Cg(Ring I)···Cg (Ring J)/Cg(I)···Me (J)	$D_p$ (Å)	$\alpha$ (°)	$\beta$ (°)	$\gamma$ (°)	$D_{1p}$ (Å)	$D_{2p}$ (Å)	Symmetry element of ring J
<b>2</b>	Cg(3)···Cg(3)	3.899(2)	0	27.70	27.70	-3.4520(16)	-3.4520(16)	$-x, -y, 1-z$
	Cg(3)···Cg(5)	3.808(2)	5.40 (19)	28.11	29.87	3.3020(16)	3.3585(17)	$-x, 1-y, -z$
	Cg(3)···Cg(6)	3.937(2)	1.1 (2)	28.94	29.19	-3.4368(16)	-3.4451(17)	$-x, -y, 1-z$
<b>3</b>	Cg(3)···Cg(5)	3.878(3)	2.3 (3)	29.20	28.33	3.414(2)	3.385(2)	$1-x, 1-y, -z$

Notes:  $\alpha$  = dihedral angle between ring I and ring J (°);  $\beta$  = angle Cg(I) → Cg(J) or Cg(I) → Me vector and normal to plane I (°);  $\gamma$  = angle Cg(I) → Cg(J) vector and normal to plane J (°);  $D_p$  = distance between the centroids of ring I and ring J;  $D_{1p}$  = perpendicular distance of Cg(I) on ring J/Cg(I)-Me(J);  $D_{2p}$  = perpendicular distance of Cg(J) on ring I/Me(J)-Cg(I). For complex **2**, Cg(3) = center of gravity of ring [N(2)-C(19)-C(18)-C(17)-C(16)-C(20)]; Cg(5) = center of gravity of ring [C(4)-C(5)-C(6)-C(7)-C(8)-C(9)]; Cg(6) = center of gravity of ring [C(12)-C(13)-C(14)-C(15)-C(16)-C(20)]. For complex **3**, Cg(3) = center of gravity of ring [N(2)-C(19)-C(18)-C(17)-C(16)-C(20)]; Cg(5) = center of gravity of ring [C(4)-C(5)-C(6)-C(7)-C(8)-C(9)].

Table 9. Geometric features of the C-H··· $\pi$  interactions in **3**.

C-H···Cg(Ring)	H···Cg (Å)	C-H···Cg (°)	C···Cg (Å)	Symmetry transformation
C(23)-H(23C)···Cg(3)	2.93	124	3.559(7)	$1/2-x, -1/2+y, 1/2-z$

Complexes **1–3** exhibit luminescence in methanol. The luminescence data, listed in table 10 (without solvent correction), are assigned as intra-ligand  $^1(\pi-\pi^*)$  fluorescence [46]. The relative quantum yields of ligands HL<sup>1</sup> and HL<sup>2</sup> and all three complexes are determined using *coumarin 6* in methanol as the reference ( $\Phi_f = 0.78$ ) at  $\lambda_{ex} = 430$  nm [47]. The quantum yields for HL<sup>1</sup> and HL<sup>2</sup> are 0.05 and 0.08, respectively. The quantum yields obtained for **1**, **2**, and **3** are 0.042, 0.065, and 0.07, respectively. The decrease in the quantum yield for complexes compared to ligands is due to the presence of paramagnetic copper(II) centers [48].

Room temperature magnetic susceptibility measurements for **1**, **2**, and **3** showed magnetic moments close to 1.73 BM, as expected for the discrete magnetically non-coupled spin-only value for copper(II), as observed in similar systems [49].

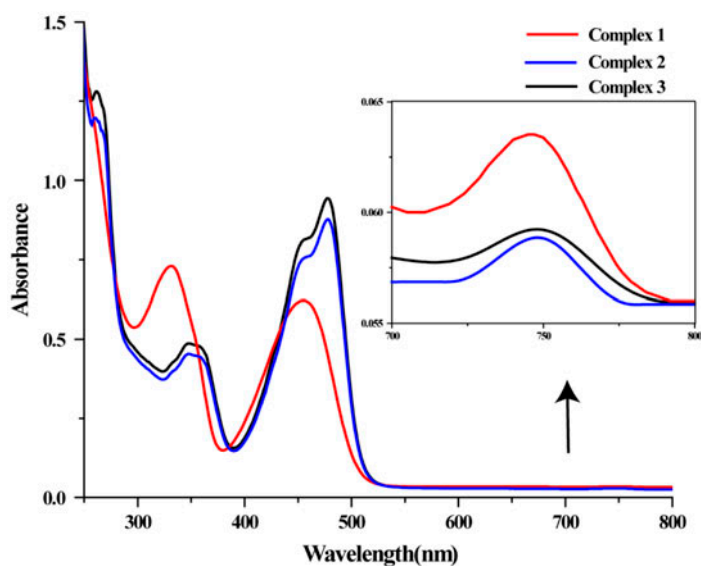


Figure 10. UV-vis spectra of the complexes in methanol.

Table 10. Photophysical data for **1**–**3**.

Complex	Absorption (nm)	Emission (nm)
<b>1</b>	336	480
<b>2</b>	348	401
<b>3</b>	348	394

#### 4. Summary

Syntheses and characterization of three new copper(II) complexes with two different tridentate  $N_2O$  donor Schiff bases,  $HL^1$  and  $HL^2$ , have been described. The supramolecular architectures of the complexes involve  $\pi \cdots \pi$ ,  $C-H \cdots \pi$ , and  $lp \cdots \pi$  interactions. The insertion of a methanol in the pendant end of ligated dicyanamide in **3** has also been observed.

#### Supplementary material

CCDC 990652, 990650, and 990651 contain the supplementary crystallographic data for **1**, **2**, and **3**, respectively. These data can be obtained free of charge via <http://www.ccdc.cam.ac.uk/conts/retrieving.html> or from the Cambridge Crystallographic Data Center, 12 Union Road, Cambridge CB2 1EZ, UK; Fax: (+44) 1223-336-033; or E-mail: [deposit@ccdc.cam.ac.uk](mailto:deposit@ccdc.cam.ac.uk).

#### Acknowledgments

P.P. Jana wishes to thank VR, the Swedish Research Council for the financial support.

## Disclosure statement

No potential conflict of interest was reported by the authors.

## Funding

This work was supported by the CSIR, India [Fellowship for Subrata Jana, Sanction No. 09/096(0659)/2010-EMR-I, dated 18.1.11]; Swedish Research Council.

## References

- [1] Z.-L. You, H.-L. Zhu. *Z. Anorg. Allg. Chem.*, **630**, 2754 (2004).
- [2] H.-P. Jia, W. Li, Z.-F. Ju, J. Zhang. *Inorg. Chem. Commun.*, **10**, 397 (2007).
- [3] J.M. Lehn. *Angew. Chem. Int. Ed.*, **27**, 89 (1988).
- [4] H.J. Schneider. *Angew. Chem. Int. Ed.*, **30**, 1417 (1991).
- [5] D.J. Braga. *J. Chem. Soc., Dalton Trans.*, 3705 (2000).
- [6] H. Li, M. Eddaoudi, M. O'Keeffe, O.M. Yaghi. *Nature*, **402**, 276 (1999).
- [7] D.J. Stufkens, A. Vleck Jr. *Coord. Chem. Rev.*, **177**, 127 (1998).
- [8] J.L. Atwood, J.E.D. Davies, D.D. MacNicol, F. Vogtle, J.M. Lehn. In *Comprehensive Supramolecular Chemistry*, J.M. Lehn (Ed.), Vols. 6 and 9, Pergamon, Oxford (1996).
- [9] M.J. Blanco, M.C. Jimenez, J.C. Chambron, V. Heitz, M. Linke, J.P. Sauvage. *Chem. Soc. Rev.*, **28**, 293 (1999).
- [10] S. Tanaka, H. Tsurugi, K. Mashima. *Coord. Chem. Rev.*, **265**, 38 (2014).
- [11] H. El Bakkali, A. Castiñeiras, I. García-Santos, J.M. González-Pérez, J. Niclós-Gutiérrez. *Cryst. Growth Des.*, **14**, 249 (2014).
- [12] M. Raynal, P. Ballester, A. Vidal-Ferran, P.W.N.M. van Leeuwen. *Chem. Soc. Rev.*, **43**, 1660 (2014).
- [13] V. Petricek, M. Dusek, L. Palatinus. *The Crystallographic Computing System, Jana 2006*, Institute of Physics, Praha (2006).
- [14] L. Palatinus, G. Chapuis. *J. Appl. Cryst.*, **40**, 786 (2007).
- [15] M.A. Spackman, D. Jayatilaka. *CrystEngComm*, **11**, 19 (2009).
- [16] F.L. Hirshfeld. *Theor. Chim. Acta*, **44**, 129 (1977).
- [17] H.F. Clausen, M.S. Chevallier, M.A. Spackman, B.B. Iversen. *New J. Chem.*, **34**, 193 (2010).
- [18] A.L. Rohl, M. Moret, W. Kaminsky, K. Claborn, J.J. McKinnon, B. Kahr. *Cryst. Growth Des.*, **8**, 4517 (2008).
- [19] A. Parkin, G. Barr, W. Dong, C.J. Gilmore, D. Jayatilaka, J.J. McKinnon, M.A. Spackman, C.C. Wilson. *CrystEngComm*, **9**, 648 (2007).
- [20] M.A. Spackman, J.J. McKinnon. *CrystEngComm*, **4**, 378 (2002).
- [21] S.K. Wolff, D.J. Grimwood, J.J. McKinnon, D. Jayatilaka, M.A. Spackman. *Crystal Explorer 2.0*, University of Western Australia, Perth (2007). Available online at: <http://hirshfeldsurfacenet.blogspot.com/>.
- [22] F.H. Allen, O. Kennard, D.G. Watson, L. Brammer, A.G. Orpen, R.J. Taylor. *J. Chem. Soc., Perkin Trans.*, **2**, S1 (1987).
- [23] J.J. Kinnon, M.A. Spackman, A.S. Mitchell. *Acta Crystallogr. B*, **60**, 627 (2004).
- [24] A.D. Becke. *J. Chem. Phys.*, **98**, 5648 (1993).
- [25] C. Lee, W. Yang, R.G. Parr. *Phys. Rev. B*, **37**, 785 (1988).
- [26] P.J. Stevens, J.F. Devlin, C.F. Chabalowski, M.J. Frisch. *J. Phys. Chem.*, **98**, 11623 (1994).
- [27] M.J. Frisch, G.W. Trucks, H.B. Schlegel, G.E. Scuseria, M.A. Robb, J.R. Cheeseman, J.A. Montgomery Jr., T. Vreven, K.N. Kudin, J.C. Burant, J.M. Millam, S.S. Iyengar, J. Tomasi, V. Barone, B. Mennucci, M. Cossi, G. Scalmani, N. Rega, G.A. Petersson, H. Nakatsuji, M. Hada, M. Ehara, K. Toyota, R. Fukuda, J. Hasegawa, M. Ishida, T. Nakajima, Y. Honda, O. Kitao, H. Nakai, M. Klene, X. Li, J.E. Knox, H.P. Hratchian, J.B. Cross, K. Raghavachari, J.B. Foresman, J.V. Ortiz, Q. Cui, M.A. Al-Laham, C.Y. Peng, A. Nanayakkara, M. Challacombe, P.M.W. Gill, B. Johnson, W. Chen, M.W. Wong, C. Gonzalez, J.A. Pople. *GAUSSIAN 03*, Revision D.01, Gaussian, Inc., Wallingford, CT (2004).
- [28] P.J. Hay, W.R. Wadt. *J. Chem. Phys.*, **82**, 270 (1985).
- [29] W.R. Wadt, P.J. Hay. *J. Chem. Phys.*, **82**, 284 (1985).
- [30] P.J. Hay, W.R. Wadt. *J. Chem. Phys.*, **82**, 299 (1985).
- [31] T. Kuroda-Sowa, Z. Yu, Y. Senzaki, K. Sugimoto, M. Maekawa, M. Munakata, S. Hayami, Y. Maeda. *Chem. Lett.*, **37**, 1216 (2008).
- [32] I.M. Atkinson, M.M. Bishop, L.F. Lindoy, S. Mahadev, P. Turner. *Chem. Commun.*, 2818 (2002).
- [33] M.M. Bishop, L.F. Lindoy, S. Mahadev, P. Turner. *J. Chem. Soc., Dalton Trans.*, **233**, (2000).
- [34] L.-L. Zheng, J.-D. Leng, W.-T. Liu, W.-X. Zhang, J.-X. Lu, M.-L. Tong. *Eur. J. Inorg. Chem.*, 4616 (2008).

- [35] X.-H. Zhao, X.-D. Chen, M. Du. *Acta Cryst.*, **E62**, m3580 (2006).
- [36] G.-F. Liu, L.-L. Li, Y. Zhang, J.-P. Lang, S.W. Ng. *Acta Cryst.*, **C63**, m1 (2007).
- [37] A.W. Addison, T. Nageswara, J. Reedijk, J. van Rijn, G.C. Verchoor. *J. Chem. Soc., Dalton Trans.*, 1349 (1984).
- [38] P. Mosae Selvakumar, S. Nadella, J. Sahoo, E. Suresh, P.S. Subramanian. *J. Coord. Chem.*, **66**, 287 (2013).
- [39] S. Nayak, P. Gamez, B. Kozlevčar, A. Pevec, O. Roubeau, S. Dehnen, J. Reedijk. *Polyhedron*, **29**, 2291 (2010).
- [40] S. Jana, P. Bhowmik, M. Das, P.P. Jana, K. Harms, S. Chattopadhyay. *Polyhedron*, **37**, 21 (2012).
- [41] M. Iqbal, S. Ali, Z.-U. Rehman, N. Muhammad, M. Sohail, V. Pandarinathan. *J. Coord. Chem.*, **67**, 1731 (2014).
- [42] M.A. Spackman, P.G. Byrom. *Chem. Phys. Lett.*, **267**, 215 (1997).
- [43] A. Bhattacharyya, S. Sen, K. Harms, S. Chattopadhyay. *Polyhedron*, **88**, 156 (2015).
- [44] P.K. Bhaumik, K. Harms, S. Chattopadhyay. *Inorg. Chim. Acta*, **405**, 400 (2013).
- [45] H.M. Park, B.N. Oh, J.H. Kim, W. Qiong, I.H. Hwang, K.-D. Jung, C. Kim, J. Kim. *Tetrahedron Lett.*, **52**, 5581 (2011).
- [46] N.J. Turro. *Pure Appl. Chem.*, **49**, 405 (1977).
- [47] S.M.Z. Al-Kindy, Z. Al-Mafrigi, M.S. Shongwe, F.E.O. Suliman. *Luminescence*, **26**, 462 (2011).
- [48] S. Basak, S. Sen, S. Banerjee, S. Mitra, G. Rosair, M.T. Garland Rodriguez. *Polyhedron*, **26**, 5104 (2007).
- [49] S. Chattopadhyay, G. Bocelli, A. Cantoni, A. Ghosh. *Inorg. Chim. Acta*, **359**, 4441 (2006).